



Applying liquisolid technique to enhance curcumin solubility: a central composite design study

Sareh Aghajanpour¹ · Shabnam Yousefi Jordehi¹ · Ali Farmoudeh¹ · Reza Negarandeh^{1,2} · Matthew Lam^{3,4} · Pedram Ebrahimnejad¹ · Ali Nokhodchi⁴ 

Received: 9 May 2024 / Accepted: 13 October 2024 / Published online: 25 October 2024
© The Author(s) 2024

Abstract

Turmeric, specifically its curcuminoids such as curcumin ($C_{21}H_{20}O_6$), possesses extensive therapeutic benefits including anti-inflammatory, anticancer, and anti-aging properties. However, curcumin's clinical effectiveness is significantly limited by its hydrophobic nature, leading to poor bioavailability. This study aims to enhance the solubility and bioavailability of curcumin through the development of liquisolid compact dispersion formulations. To address curcumin's limited water solubility (3.12 mg/l at 25 °C) and high oil–water partition coefficient ($\log K_{ow} = 3.29$), we employed a central composite design (CCD) to optimize liquisolid compact dispersion formulations. The optimization focused on the tablet's physical properties, such as hardness, disintegration time, and dissolution rate at 30 min. Critical formulation components included Tween 80 as the liquid vehicle and Aerosil 200 as the coating material, serving as independent variables in the optimization process. The optimized formulation, containing 30 mg of Tween 80 and 75 mg of Aerosil 200, significantly improved curcumin's dissolution rate. Experimental results confirmed the formulation's effectiveness, with a marked reduction in the time to dissolve 63.2% of the drug to 165 min, compared to 300 min for conventional formulations. Differential scanning calorimetry and Fourier-transform infrared spectra indicated a transformation of curcumin into a non-crystalline state and the formation of hydrogen bonds with Tween 80, contributing to enhanced solubility. This study successfully demonstrates a viable strategy to enhance the bioavailability of curcumin through liquisolid compact dispersion formulations. By addressing the solubility challenges of curcumin, this technique presents a significant advancement in improving the clinical applicability of BCS class II and IV drugs, potentially benefiting a wide range of therapeutic applications.

✉ Pedram Ebrahimnejad
pebrahimnejad@mazums.ac.ir

✉ Ali Nokhodchi
a.nokhodchi@sussex.ac.uk

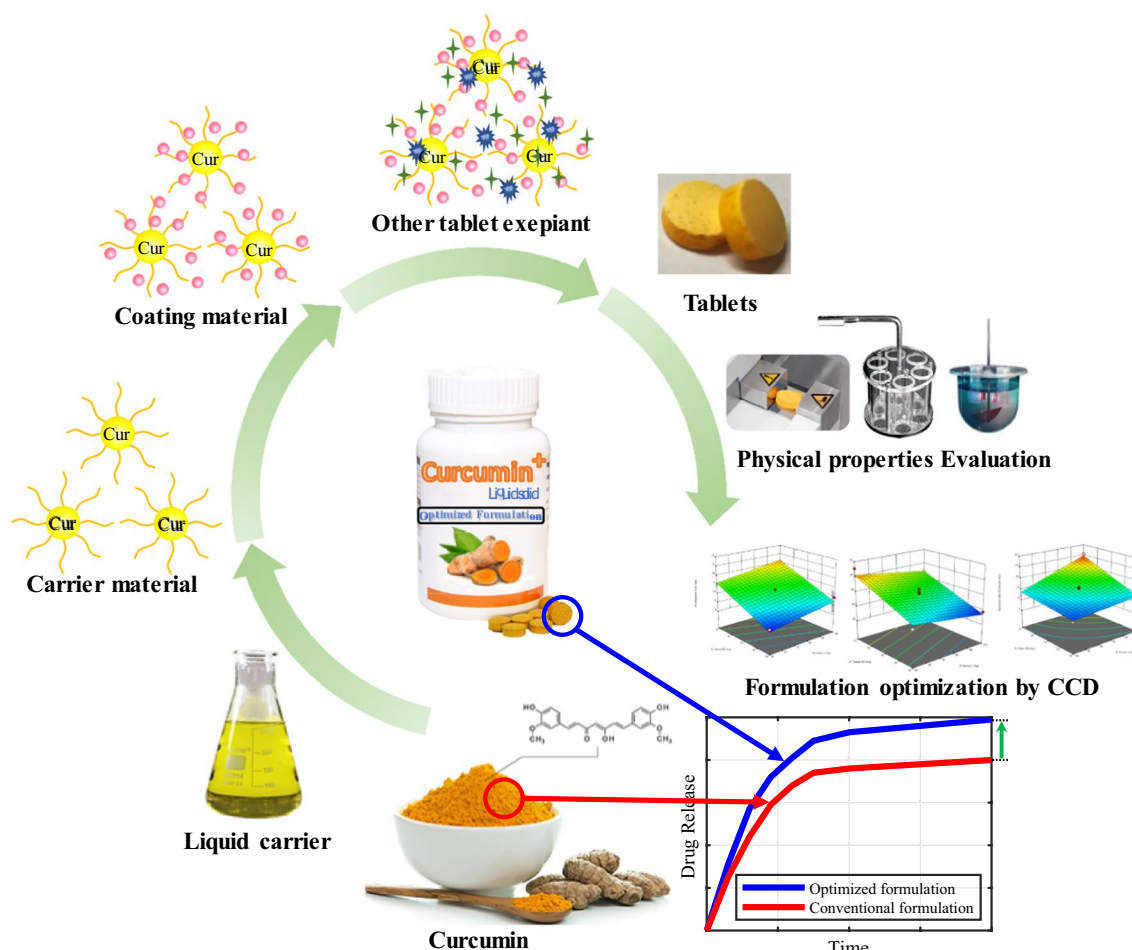
¹ Department of Pharmaceutics, Faculty of Pharmacy,
Mazandaran University of Medical Sciences, Sari, Iran

² Student Research Committee Center, Mazandaran University
of Medical Sciences, Sari, Iran

³ Department of Chemical and Pharmaceutical Sciences,
School of Human Sciences, London Metropolitan University,
166-220 Holloway Road, London N7 8DB, UK

⁴ School of Life Sciences, University of Sussex, Brighton, UK

Graphical abstract



Graphical representation of optimizing curcumin liquisolid formulation using central composite design (CCD) methodology

Keywords Liquisolid tablet · Bioavailability · Powder solution technology · Curcumin · Central composite design

Introduction

Curcumin, a yellow-colored extract derived from the turmeric rhizome (*Curcuma longae rhizoma*), has been a staple of traditional medicine for centuries. It is the primary and most extensively studied compound among the curcuminoids, a group of dimeric derivatives of ferulic acid commonly found in Indian cuisine (Górnicka et al. 2023). Curcuminoids are known chemically as diferuloylmethane with the IUPAC name (1E,6E)-1,7-Bis(4-hydroxy-3-methoxyphenyl) hepta-1,6-diene-3,5-dione. Its chemical formula is $C_{21}H_{20}O_6$, and it has a molecular weight of 368.385 g/mol, a log Kow of 3.29, and a melting point of around 182 °C (Fig. 1) (Obeid et al. 2023).

Several studies have demonstrated that curcumin possesses a range of beneficial effects, namely antioxidant

(Kumar et al. 2016), anti-inflammatory (Basnet and Skalko-Basnet 2011), antibacterial (Negi et al. 1999), antiviral (Hewlings and Kalman 2017), immunomodulatory (Yang et al. 2020; Abo-Zaid et al. 2020), and anticancer properties (Giordano and Tommonaro 2019). Consequently, it has attracted considerable attention for its potential therapeutic benefits in various conditions, such as arthritis, liver diseases, diabetes, neurodegenerative diseases, obesity, and cardiovascular issues (Hewlings and Kalman 2017; Harthogh et al. 2020; Yan et al. 2017; Hamaguchi et al. 2010; Nabavi et al. 2014; Hu et al. 2018; Rathore et al. 2020). As a result, curcumin has become a focal point of interest in the scientific community due to its diverse biological activities and potential therapeutic applications.

Although curcumin has been proven to have many pharmacological effects, its clinical application is hindered by its

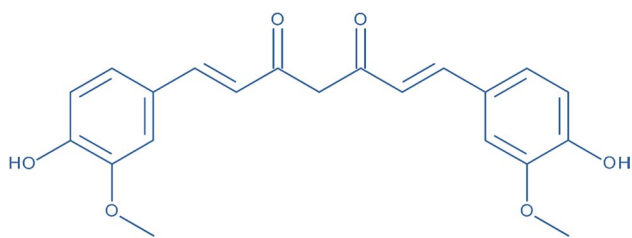


Fig. 1 Structural formula of curcumin

poor water solubility (3.12 mg/l at 25 °C) and hydrophobicity, making it not very effective (Rathore et al. 2020). The poor solubility of curcumin is a significant concern as it leads to low bioavailability, resulting in poor absorption in the circulatory system and target tissues. The limited solubility of curcumin in water means that its concentration in serum does not exceed 60 nmol/L. Furthermore, a notable portion of curcumin undergoes inactivation during the liver metabolism process, resulting in the highest concentration of curcumin in the body typically being observed 1–2 h after oral consumption. Additionally, curcumin exhibits photosensitivity and experiences constrained chemical stability throughout the manufacturing and storage processes (Anand et al. 2007).

Drawing from previous studies, the liquisolid method emerges as a comprehensive solution for enhancing the dissolution rate and bioavailability of BCS Class II and IV drugs like curcumin (Kala et al. 2014; Souza Ferreira and Bruschi 2019; Kumar et al. 2019). The liquisolid technique, pioneered by Spireas (Spireas and Sadu 1998), suggests dispersing lipophilic drugs in a suitable non-volatile liquid vehicle, such as polyethylene glycol, Tween 20 and Tween 80. As the presence of liquid vehicles can reduce the flowability of liquid–powder admixture (Spireas and Sadu 1998), therefore, coating material is necessary to cover the surface of the particles, thereby maintaining the powder's flowability. Dispersed drug particles are typically presented in a minimized size, resulting in an enhanced dissolution rate. Moreover, the liquisolid approach holds significant promise due to its straightforward manufacturing process and cost-effectiveness.

In several studies, essential properties of liquisolid tablets, such as tablet hardness, disintegration, and in vitro drug release, showed significant improvement through the adjustment of variables like the liquid vehicle and coating material (Saeedi et al. 2022). However, the development and optimization of such formulations are often conducted through a trial-and-error method, involving the alteration of one factor while keeping other factors constant. This univariate approach is time-consuming and demands numerous experiments to elucidate the impact of excipients on the physical attributes of the liquisolid formulation (Tiong and Elkordy

2009). Furthermore, it frequently falls short in projecting the true optimal composition due to the neglect of interactions between factors. Central composite design (CCD) is a key subset of response surface methodology (RSM) that presents a robust and novel solution to explore the complex relationship between formulation variables and product quality. In regression analysis, model building is the process of developing a probabilistic model that best describes the relationship between the dependent and independent variables. When the variables are measurable, continuous and controllable through designed experiments with no statistically significant errors, CCD can be utilized to create the model and optimize the process. This involves conducting a series of experimental runs to accurately and reliably measure these response variables with best-of-fit, and finally determining the optimal set of experimental parameters to produce the optimal response value (Choiri et al. 2018; Biswas et al. 2017; Beg et al. 2017; Ainurofiq et al. 2016). Systematic optimization of pharmaceutical products utilizing CCD necessitates fewer trial runs and is adept at uncovering potential synergies or interactions among components, ultimately yielding a robust formulation and potential savings in terms of time, cost and developmental effort.

In recent years, various methods such as liposome preparation, niosomes and the use of co-solvents have been utilized to improve the dissolution rate and bioavailability of curcumin (Ghadi and Ebrahimnejad 2017; Ghadi et al. 2019; Sadeghi-Ghadi and Ebrahimnejad 2019; Sadeghi-Ghadi et al. 2020; Hezarjaribi et al. 2022; Sadeghi-Ghadi et al. 2023; Ahmadi et al. 2023). Among them, the liquisolid technique stands out as a promising option due to its benefits such as cost-effectiveness and ease of processing. Therefore, the current study aims to establish a robust liquisolid system for curcumin by systematically optimizing tablet hardness, disintegration, and dissolution at 30 min using the CCD method. This endeavor seeks to produce a curcumin liquisolid formulation based on solvent and coating material, to significantly enhance curcumin's pharmaceutical properties for the development of a high-bioavailability liquisolid system.

Experimental

Materials

Curcumin, Aerosil 200, potassium dihydrogen phosphate, sodium hydroxide, magnesium stearate, propylene glycol, and PVP K25 were obtained from Merck (Germany). Avicel PH 102, or microcrystalline cellulose (MCC), was provided by FMC Pharmaceuticals in Ireland. Tween 20, 60, and 80 were purchased from Samchun (Korea). All other chemicals were of analytical grade.

Phase-solubility studies

An excess amount of curcumin was added to 30 mL of distilled water. The mixture was shaken for 24 h at 25 ± 1 °C in a thermostatic water bath (7500S, Pars Nahand ENGG. CO, Iran). The resulting curcumin suspensions were filtered through a Millipore filter (0.45 μm) and centrifuged at 15,000 rpm for 15 min (Z 36 HK, HERMLE, Germany). The resulting supernatant was suitably diluted, and UV absorption was recorded at 428 nm using a spectrophotometer (Bio-wave II UV, Biochrome Ltd., Cambridge CB4 OF England) (Ghadi et al. 2019). The solubility of curcumin in liquid vehicles containing propylene glycol, Tween 20, Tween 60, and Tween 80 were also determined using the same method to evaluate the most effective solvent.

Determination of flow properties

Powders consisting of Avicel and Aerosil 200 were meticulously weighed and gradually blended with one of the specified liquid medications using a mortar and pestle. This meticulous blending process was conducted to attain optimal flowability and compactibility for the liquisolid formulation. Subsequently, the resulting liquisolid powders underwent a comprehensive powder flow test, which included the assessment based on the liquid load factor (L_f), Carr's index (CI), Hausner's ratio (HR), and angle of repose (θ).

The amounts of excipients required to prepare liquisolid formulations with acceptable flow properties, referred to as L_f (liquid load factor), are defined as the ratio between the weight of liquid medication (W) and the carrier (Q) (Wei and Manickam 2012):

$$L_f = \frac{W}{Q}. \quad (1)$$

CI was calculated using the bulk (ρ_b) and tapped density (ρ_t) data:

$$CI = \frac{\rho_t - \rho_b}{\rho_t} \times 100. \quad (2)$$

Similarly, HR was determined using:

$$HR = \frac{\rho_t}{\rho_b}. \quad (3)$$

Lower values of CI and HR indicate better powder flowability. The other method employed for characterizing flowability was the measurement of the θ . The angle of repose was calculated using the fixed funnel and free-standing cone method. The θ was calculated as:

$$\theta = \tan^{-1} \left(\frac{2h}{d} \right), \quad (4)$$

where d represents the average diameter of the formed cone, and h denotes the height of the pile.

Preparation of liquisolid compacts

A series of curcumin liquisolid formulations denoted as F1 to F11 were carefully crafted. In this process, curcumin was initially dispersed in a non-volatile liquid vehicle (Tween 80) using a mortar and pestle. Following this, the carrier material (Avicel) and the coating substance (Aerosil 200) were methodically introduced. After thorough mixing, PVP (a binder) and magnesium stearate (a lubricant) were added and blended for 2 min. Subsequently, the resulting powder blend was compacted using a single-punch eccentric tablet press machine (Korsch Pressen, Germany) to prepare liquisolid tablets. The employed flat-faced punch, featuring a diameter of 14.5 mm, was selected to regulate tablet hardness within the range of 35 to 65 N. This deliberate choice of hardness range was made to ensure that all liquisolid compacts met the predetermined criterion with precision.

Physical characterization of tablets

Weight variation assessment

From each batch, twenty tablets were randomly chosen and individually weighed on an electronic balance (GF-600, A&D®, Japan). The average weight and standard deviation for each batch of tablets were calculated.

Hardness

Six tablets of each formulation were placed in a hardness tester (TBH 30 MD, Erweka, Germany), and the force required to crush each was recorded. This approach is in accordance with the compendial requirement for testing tablet hardness (United States Pharmacopeia 2022).

Friability

The friability of each formulation was determined using a friability tester (Erweka, Germany). To this end, 30 tablets, equivalent to 6.5 g, were accurately weighed and placed in the friability tester. The tester was operated at 25 rpm for

Table 1 Independent variables in actual and coded levels

| Independent variables | Symbol | Levels | | |
|--------------------------|--------|--------|----|-----|
| | | -1 | 0 | 1 |
| $X_1 =$ Tween 80 (mg) | A | 10 | 30 | 50 |
| $X_2 =$ Aerosil 200 (mg) | B | 50 | 75 | 100 |

Table 2 Independent variables and responses data for central composite design (data shown as mean \pm standard deviation, $n = 3$)

| Formulation code | Independent variables | | | Responses | |
|------------------|-----------------------|------------------|-------------------|---------------------------|---------------------------|
| | Tween80 (mg) | Aerosil 200 (mg) | Hardness (newton) | Disintegration time (min) | Dissolution at 30 min (%) |
| 1 | 58 | 75 | 36.27 \pm 1.1 | 6.54 \pm 0.27 | 21.15 \pm 0.18 |
| 2 | 10 | 50 | 65.53 \pm 4.34 | 11.67 \pm 0.25 | 14.93 \pm 0.75 |
| 3 | 30 | 75 | 50.97 \pm 1.31 | 9.86 \pm 0.44 | 16.55 \pm 0.68 |
| 4 | 30 | 75 | 52.93 \pm 1.00 | 11.26 \pm 0.47 | 15.31 \pm 1.12 |
| 5 | 30 | 110 | 41.83 \pm 2.67 | 11.68 \pm 0.23 | 12.52 \pm 1.06 |
| 6 | 2 | 75 | 57.30 \pm 2.09 | 16.14 \pm 0.25 | 9.87 \pm 1.02 |
| 7 | 50 | 50 | 41.43 \pm 1.29 | 7.24 \pm 0.30 | 25.42 \pm 1.13 |
| 8 | 30 | 40 | 51.23 \pm 1.32 | 9.20 \pm 0.21 | 18.29 \pm 1.46 |
| 9 | 30 | 75 | 50.03 \pm 1.75 | 9.25 \pm 0.11 | 16.02 \pm 0.89 |
| 10 | 10 | 100 | 54.27 \pm 3.36 | 14.29 \pm 0.19 | 10.38 \pm 0.32 |
| 11 | 50 | 100 | 38.60 \pm 1.55 | 9.85 \pm 0.21 | 12.09 \pm 0.94 |
| 12* | – | – | 61.72 \pm 1.53 | 16.96 \pm 0.23 | 12.73 \pm 0.23 |

*F12 is conventional formulation

4 min, corresponding to 100 revolutions. After the test, the tablets were dedusted and reweighed. The friability is determined using Eq. (5).

$$\text{Friability}(\%) = \frac{W_{\text{initial}} - W_{\text{final}}}{W_{\text{initial}}} \times 100, \quad (5)$$

where W_{initial} is the initial weight of the tablets and W_{final} is the weight of the tablets after the friability test (United States Pharmacopeial Convention (2020)). According to the criteria outlined in the US Pharmacopeia standards, tablets are deemed acceptable if they show less than 1% weight loss and remain intact with no cracks, splits, or breakages (United States Pharmacopeial Convention 2019).

Disintegration

The disintegration time of curcumin liquisolid tablets was measured using a tablet disintegration apparatus (type ZT 121, Erweka, Germany). The apparatus consisted of a basket rack assembly that moves along the vertical axis in 1 L of water with a temperature of 37 ± 2 °C. Six tablets from each formulation were placed in the basket and the time taken for the complete disintegration of the tablet was recorded (United States Pharmacopeial Convention 2019).

Content uniformity

To determine the drug content, liquisolid tablets equivalent to 5 mg of curcumin were pulverized using a mortar and pestle. The resulting powder was then extracted with ethanol, leveraging previous studies that confirmed the solubility of

curcumin in ethanol as 10 mg/ml (Cui et al. 2021; Li et al. 2023). The obtained extract was then passed through Whatman filter paper (0.45 μ m), and the filtrates were analyzed using UV/Vis spectrophotometry at a wavelength of 428 nm to quantify the drug content.

In vitro dissolution studies

The dissolution test was conducted using a USP II paddle apparatus (Erweka, Germany). The experiments were performed in 900 ml of a phosphate buffer solution with a pH of 6.8 at a controlled temperature of 37 ± 0.5 °C. The paddle rotation speed was set at 50 rpm. At specific time intervals, samples were withdrawn and analyzed using spectrophotometry at 428 nm. To maintain a constant volume, the withdrawn volume was immediately replenished with an equal volume of fresh dissolution medium. The obtained dissolution profile can provide insights into the release behavior of the optimized formulation (Ravichandran 2013).

Design of the experiments using CCD

To attain the optimal liquisolid formulation, attempts were made to enhance key physical characteristics of the tablet, including tablet hardness, disintegration time, and dissolution at 30 min. This was achieved by varying the amounts of the liquid vehicle and coating material as key variables. In this study, a two-factor, three-level CCD was employed to cover 11 experiments to optimize the formulation variables for curcumin liquisolid. Our CCD goal was to optimize the formulation by focusing on three critical parameters: tablet hardness

Fig. 2 Solubility of curcumin in various solvents (data shown as mean \pm standard deviation, $n = 3$)

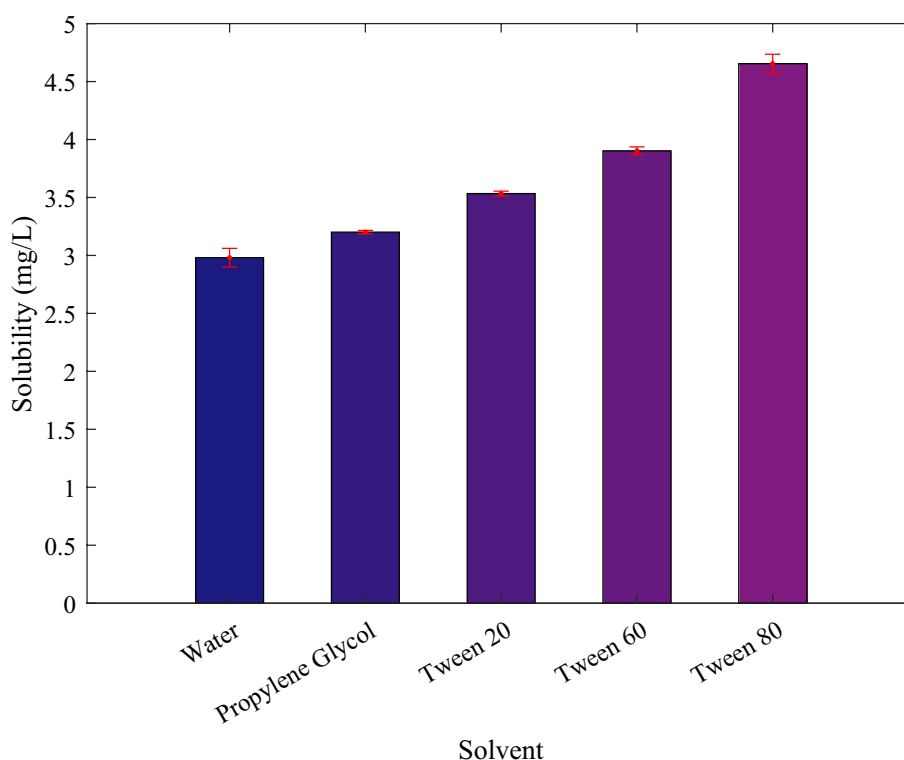


Table 3 Hardness, Hausner's ratio, car's percent, disintegration time, content uniformity and weight variation of curcumin liquisolid

| Formulation code | Hardness (N) | Hausner's ratio | Car's Index (%) | Angle of repose (°) | Disintegration time (min) | Content uniformity (%) | Weight variation (mg) |
|------------------|------------------|------------------|------------------|---------------------|---------------------------|------------------------|-----------------------|
| 1 | 36.27 \pm 1.10 | 1.10 \pm 0.008 | 9.33 \pm 0.67 | 31.79 \pm 0.83 | 6.54 \pm 0.27 | 99.17 \pm 1.06 | 496.74 \pm 5.63 |
| 2 | 65.53 \pm 4.34 | 1.07 \pm 0.004 | 6.88 \pm 0.41 | 28.96 \pm 0.56 | 11.66 \pm 0.25 | 96.93 \pm 2.27 | 498.67 \pm 0.36 |
| 3 | 50.97 \pm 1.30 | 1.08 \pm 0.005 | 7.77 \pm 0.36 | 28.96 \pm 0.51 | 9.86 \pm 0.44 | 96.90 \pm 2.87 | 496.98 \pm 7.21 |
| 4 | 52.93 \pm 1.00 | 1.09 \pm 0.003 | 8.00 \pm 0.12 | 29.25 \pm 0.21 | 10.76 \pm 0.04 | 99.27 \pm 1.35 | 499.01 \pm 3.98 |
| 5 | 41.83 \pm 2.67 | 1.05 \pm 0.011 | 4.44 \pm 0.98 | 26.56 \pm 0.92 | 11.67 \pm 0.23 | 97.77 \pm 2.06 | 497.48 \pm 1.05 |
| 6 | 57.30 \pm 2.09 | 1.04 \pm 0.004 | 4.22 \pm 0.29 | 25.64 \pm 0.09 | 16.14 \pm 0.25 | 96.63 \pm 1.51 | 497.15 \pm 1.74 |
| 7 | 41.43 \pm 1.29 | 1.11 \pm 0.013 | 10.22 \pm 1.02 | 30.11 \pm 0.14 | 7.24 \pm 0.30 | 99.25 \pm 1.35 | 500.10 \pm 2.82 |
| 8 | 51.23 \pm 1.32 | 1.11 \pm 0.005 | 10.22 \pm 0.38 | 30.96 \pm 0.48 | 9.20 \pm 0.21 | 98.42 \pm 0.34 | 498.29 \pm 3.36 |
| 9 | 50.03 \pm 1.75 | 1.08 \pm 0.009 | 7.33 \pm 0.59 | 28.37 \pm 0.51 | 10.12 \pm 0.15 | 99.53 \pm 0.62 | 498.44 \pm 6.43 |
| 10 | 54.27 \pm 3.36 | 1.03 \pm 0.007 | 2.66 \pm 0.67 | 23.75 \pm 0.95 | 14.29 \pm 0.19 | 98.39 \pm 1.50 | 498.82 \pm 5.07 |
| 11 | 38.60 \pm 1.55 | 1.05 \pm 0.015 | 4.88 \pm 1.39 | 26.56 \pm 0.53 | 9.85 \pm 0.20 | 97.80 \pm 1.95 | 500.13 \pm 3.68 |
| 12* | 61.72 \pm 1.53 | 1.05 \pm 0.007 | 4.67 \pm 0.63 | 23.79 \pm 0.47 | 16.96 \pm 0.23 | 98.13 \pm 1.53 | 499.29 \pm 3.76 |

*F12 is conventional formulation

(Y_1), disintegration time (Y_2), and 30-min dissolution rate (Y_3). The chosen independent variables, Tween 80 (X_1) and Aerosil 200 (X_2), were determined at three different levels coded as -1, 0, and +1 (Table 1). The experiment matrix provided in Table 2 outlines the setup for a CCD which was implemented to investigate the main effects of the two variables on critical

responses, including tablet hardness, disintegration time, and dissolution at 30 min. These experiments incorporated factorial points, axial points, and three replicated center points, essential for estimating the sum of square errors.

The total number of experiments included $2^k + 2k + cp$ experiments, where k represents the number of independent

variables and cp denotes the number of central points. It should be noted that all formulations contain 30 mg curcumin, 25 mg PVP K25, and 5 mg magnesium stearate plus various concentrations of Tween 80 and Aerosil 200 which are listed in Table 2. Furthermore, to mitigate systematic errors, the sequence of experiments was randomized. The two-factor interaction model derived from the design is represented by Eq. (6):

$$Y_i = b_0 + b_1X_1 + b_2X_2 + b_{12}X_1X_2 + b_{11}X_1^2 + b_{22}X_2^2, \quad (6)$$

where Y_i is the dependent variable; b_0 is the intercept (arithmetic mean response of runs); b_1 , b_2 , b_{11} , b_{12} , and b_{22} are the regression coefficients. In addition, X_1 and X_2 are the independent variables.

The experimental designs and regression analysis of the data were performed using Design-Expert® V10.0.1 software (Stat-Ease, Inc., Minneapolis, MN). To assess the significance of the data, an analysis of variance (ANOVA) was conducted. Perturbation and three-dimensional (3D) surface plots were generated to visually depict the effects of the factors on the responses. The coefficient of multiple determination (R^2) value was utilized to indicate the variance described by the model.

Differential scanning calorimetry (DSC)

The thermal behavior and solid state of the liquisolid formulations were evaluated using a DSC (pyris6, PerkinElmer, USA). For analysis, roughly 5 mg of the sample was deposited into a perforated aluminum sealed pan. The analysis was performed under dry nitrogen purging, employing a heating rate of 10 °C/min within a covering temperature range of 30–300 °C (Sanka et al. 2014).

Fourier transformed infrared (FTIR) spectroscopy

To investigate potential interactions between the drug and the carrier in the solid state, Fourier transformed infrared (FTIR) spectroscopy was employed. Spectra were acquired using an FTIR spectrophotometer (FTIR-One, PerkinElmer, USA) utilizing the conventional KBr pellet method (Solanki et al. 2012). Measurements were conducted within a frequency range of 450–4000 cm^{-1} with a resolution of 1 cm^{-1} .

Statistical analysis of data

Data underwent statistical analysis, involving a T test to assess mean differences between two groups and ANOVA for comparisons involving three or more groups. Significance

was established at a $P < 0.05$. Following ANOVA, a Student–Newman–Keuls test was employed to pinpoint the specific group exhibiting significant divergence from the rest.

Results and discussion

Solubility studies

The solubility of curcumin in several co-solvents is present in Fig. 2. It can be seen that the drug was more soluble in Tween 80 (4.65 mg/L) than in others co-solvents, which is in line with the results observed by Sharma and Pathak (Sharma and Pathak 2016). Thus, Tween 80 was selected as the liquid vehicle in the formulation of the liquisolid system.

Evaluation of quality and performance of formulations

In the evaluation of curcumin liquisolid tablets, various tests were conducted to assess the key factors related to the quality and performance of the tablets. Table 3 provides an overview of the results obtained for liquisolid formulations in terms of tablet hardness, disintegration time, content uniformity, weight variation and flowability (Hausner's ratio, Carr's index and angle of repose). The results indicated that the powder exhibited suitable flowability as shown in Table 3, where all formulations exhibited excellent or good flowability. Table 3 also indicated that the tablets of all formulations exhibited a hardness within the range of 35–65 N, demonstrating their favorable strength.

The friability test showed that all tablet formulations exhibited friability values of less than 1%, meeting the USP criteria. This indicates that the tablets were able to withstand mechanical stress without significant physical damage during handling, packaging and shipping. The disintegration time, a critical factor influencing the dissolution and drug release properties of the tablets, was examined for all formulations. The disintegration time ranged from 6 to 17 min which was within the acceptable range set by the USP for uncoated regular tablets (Table 3). This suggests that the tablets had the potential for rapid disintegration and drug release.

Furthermore, the content uniformity test was conducted according to the USP guidelines to assess the consistency of the drug content in the tablets. The results revealed that the content of curcumin in all tablets fell within the acceptable range of 85% to 115%, indicating uniformity in the formulation. In summary, the evaluation of curcumin liquisolid tablets involved a comprehensive assessment of various parameters. The results from the tablet hardness, friability, flowability, disintegration time, content uniformity, and weight variation tests indicate that the prepared tablets

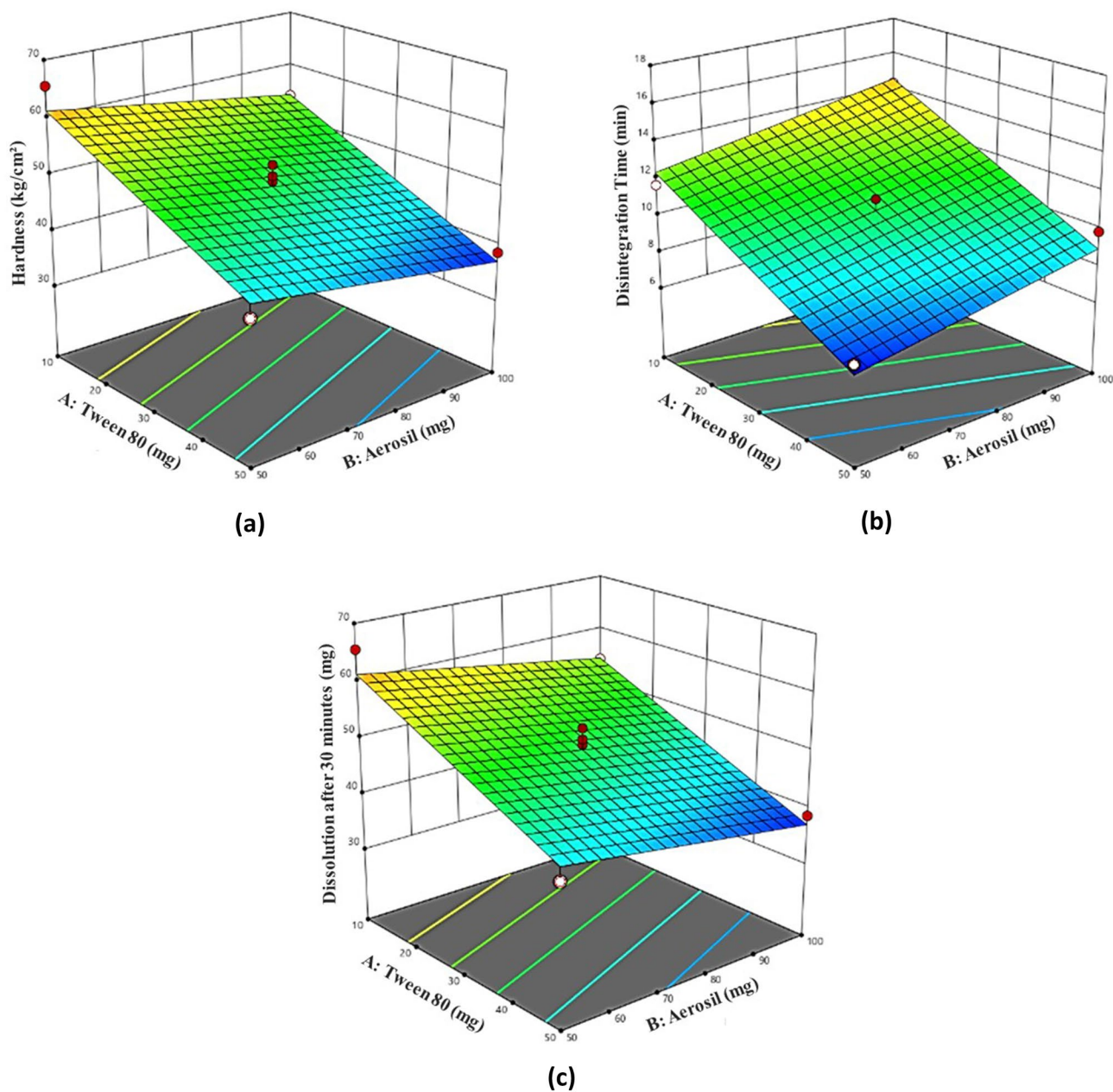


Fig. 3 3D surface graphs showing the effect of cosolvent and Aerosil 200 on **a** Hardness, **b** Disintegration Time, and **c** Dissolution at 30 min

possessed appropriate strength, flow properties, disintegration properties, and excellent content uniformity. These findings underscore the successful formulation of a robust dosage form that meets quality control requirements.

Optimization by CCD statistical technique

The optimization process was conducted using CCD design, which utilized RSM. The CCD design presented a linear relationship between the variables and tablet hardness. A

linear relationship between Tween 80 (A), Aerosil 200 (B) and tablet hardness is shown in Eq. (7).

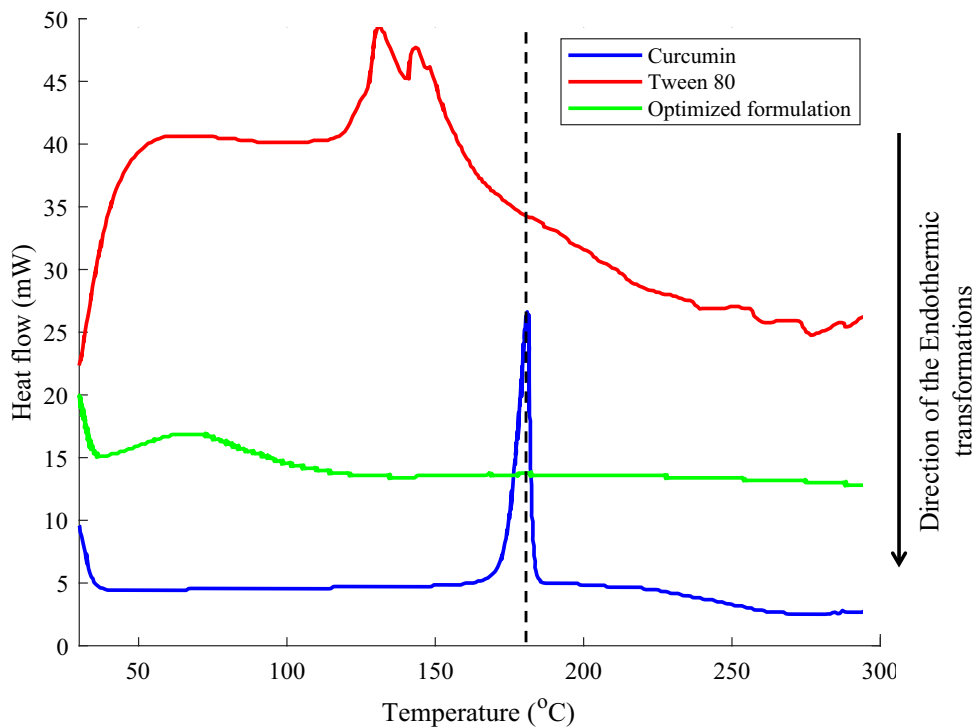
$$\text{Hardness} = +49.13 - 8.69A - 3.42B \quad (7)$$

The linear model best fitted to the experimental data with a p -value < 0.001 and the lack of fit p -value was 0.162. It can be seen that increasing each variable results in a decrease in tablet hardness. The findings are also shown in Fig. 3a.

Moreover, the coefficients (8.69 over 3.42) underscore that changes in Tween 80 (parameter A) had a more significant impact on tablet hardness. This can be explained

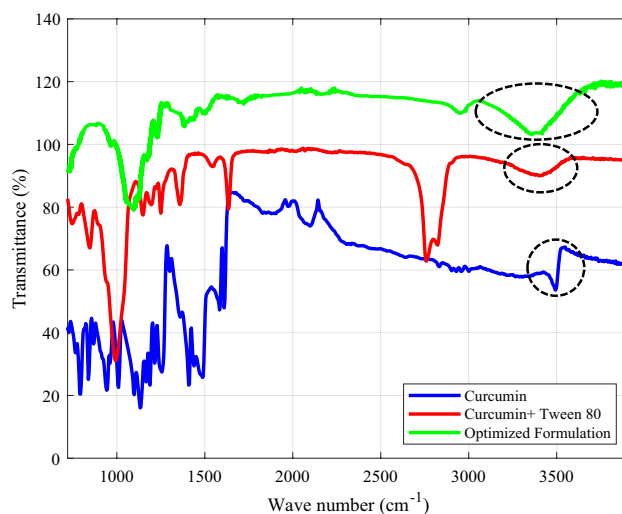
Table 4 Point predictions with 95% confidence interval

| Response | Predicted mean | Predicted median | Std Dev | SE mean | 95% CI low for mean | 95% CI high for mean | 95% TI low for 99% Pop | 95% TI high for 99% Pop |
|---------------------------|----------------|------------------|---------|---------|---------------------|----------------------|------------------------|-------------------------|
| Hardness (N) | 49.13 | 49.13 | 3.09 | 0.93 | 46.98 | 51.27 | 33.7828 | 64.47 |
| Disintegration Time (min) | 10.63 | 10.63 | 0.95 | 0.29 | 9.98 | 11.29 | 5.93 | 15.34 |
| Dissolution at 30 min (%) | 15.68 | 15.68 | 1.45 | 0.438 | 14.64 | 16.72 | 8.13 | 23.24 |

Fig. 4 Heating curves of DSC for curcumin, Tween80, and optimized formulation (F4), which contains 30 mg of Tween 80 and 75 mg of Aerosil 200

by observing that an increase in the amount of surfactant in the tablets led to a reduction in the hardness of tablets, a finding that is in line with earlier studies (Heng et al. 1990). Sander et al. (2009) illustrated that during the compression of liquid admixture, tablet hardness diminishes as non-volatile liquid increases, which is particularly noticeable when the liquid load is relatively high. Regarding Aerosil 200 (parameter B), its negative impact on tablet hardness can be attributed to its hydrophilic nature, along with two other mechanisms. First, Aerosil reduces the contact points between primary particles, potentially leading to weaker bonding within the tablet matrix. This reduction in inter-particle bonding can result in a reduction in tensile strength and hardness of the tablet. Second, Aerosil may exhibit lubricating properties. At high concentrations, lubricants can form a film over particle surfaces, hindering the formation of strong bonds during compression (Ohta et al. 2003; Esezobo 1985).

The relation between the independent and dependent variables was additionally clarified through contour plots and

**Fig. 5** FTIR spectra of curcumin, curcumin+ Tween 80, and optimized formulation

three-dimensional RSM plots shown in Fig. 3. The impacts of Tween 80 and Aerosil 200 on tablet hardness are illustrated in Fig. 3a.

For effective drug absorption, the tablet needs to undergo disintegration, which can increase the surface area available for efficient drug dissolution in the gastrointestinal fluid. Therefore, the process of tablet disintegration significantly affects the drug's dissolution. To derive a relationship between the independent variables and disintegration time, the software examined different mathematical models, and the following linear model Eq. (8) was the best-fitted model (p -value < 0.001, lack of fit p -value = 0.651).

$$\text{Disintegration time} = +10.63 - 2.81A + 1.09B \quad (8)$$

Equation 8 demonstrates that increasing Tween 80 (parameter A) concentration (parameter A) decreases disintegration time, with a negative coefficient of $-2.81 A$. In contrast, increasing Aerosil 200 (parameter B) concentration leads to longer disintegration times, as shown by a positive coefficient of $+1.09 B$. The coefficients suggest that the effect of Tween 80 (parameter A) on reducing disintegration time is more than twice as pronounced compared to the effect of increasing Aerosil 200 (parameter B) concentration.

Tablets with high hardness are typically associated with longer disintegration times or reduced propensity for disintegration t_{50} . Additionally, disintegration time can be influenced by other physical properties, such as tablet porosity and pore structure. Tablets with enhanced hardness or those manufactured under high compression forces will have smaller pores, requiring more time for water penetration into the tablet and resulting in prolonged disintegration times

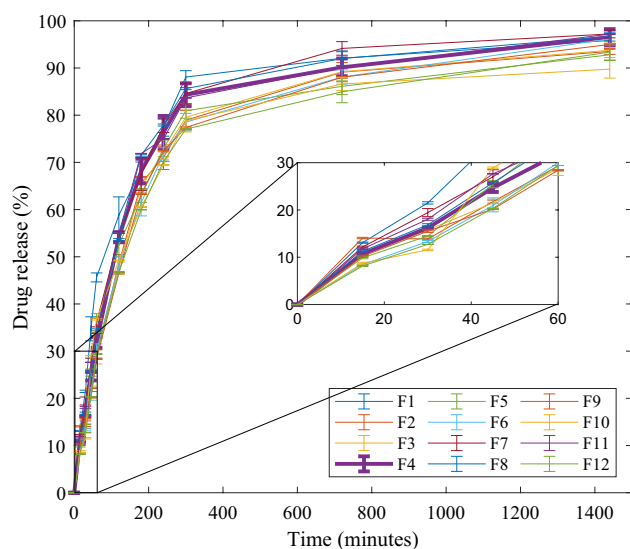


Fig. 6 In vitro drug release profile of liquisolid formulations (F1-F11) and the conventional (F12) formulation in PH = 6.8

(Juppo et al. 1991; Parrott et al. 1981). As mentioned above, increasing Tween 80 could decrease hardness, thereby potentially reducing disintegration time is reasonable. Conversely, the increased use of Aerosil 200 (parameter B) in the formulation correlates with longer tablet disintegration times, which aligns with previous studies (Esezobo 1985). This effect could be attributed to the fine particle size and large surface area of Aerosil 200. Despite its hydrophilic nature, which aids in attracting water, the resultant dense and cohesive structure may slow down the disintegration process. These findings are depicted in three-dimensional RSM plots of Fig. 3b as well.

Dissolution after 30 min was the most important parameter of our study to evaluate the drug release performance of curcumin in liquisolid formulation which was considered as a final response in CCD statistical analysis. The Eq. (1) obtained for dissolution is a quadratic model and is the best-fitted model to the experimental data with a p -value < 0.001 and the lack of fit p -value was 0.126.

$$\text{Dissolution after 30 minute} = +15.68 + 3.52A - 3.26B - 2.2AB \quad (9)$$

This equation elucidates the influence of Tween 80 (parameter A) and Aerosil 200 (parameter B) as well as their interaction on drug dissolution within 30 min. The model indicates that Tween 80 (parameter A) enhances drug dissolution after 30 min, while Aerosil 200 (parameter B) is associated with a negative coefficient, signifying that an increase in Aerosil 200 amount results in a reduction in the dissolution rate within the specified time frame. These findings can be rationalized by considering their impact on disintegration time, as outlined in Eq. 8. Additionally, the final term of Eq. 9 denotes an interaction between variables A and B, indicating that the effect of one variable is contingent on the level of the other. These observations are illustrated in the three-dimensional RSM plots presented in Fig. 3c.

CCD also predicted the optimized formulation based on the experimental data. It was observed that the values of the optimum variables level were the same as the central point ($A = 30$, $B = 75$). As a result, it can be assumed that the predicted answers are similar to the central point (Table 4).

DSC and FTIR

DSC was employed to investigate the solid state of the curcumin in the formulation. As depicted in Fig. 4, the pure curcumin thermogram displayed a sharp peak at 182.4 °C, indicating its melting point. In the DSC traces of the liquisolid formulation, the characteristic peak of curcumin was not observed, which reveals that the drug is not in the crystalline state and is dispersed molecularly in the Tween 80. These findings are consistent with previous research (United States Pharmacopeial Convention 2019).

Table 5 In vitro drug release kinetics parameters of optimized formulation and F12

| | Formula | Factor | Optimized formulation | F12 |
|------------------|---|--------|-----------------------|---------|
| Korsmeyer–Peppas | $\log(Q_t/Q_0) = \log K + n \log t$ | R^2 | 0.986 | 0.985 |
| | | RMSE | 4.441 | 3.803 |
| | | n | 0.723 | 0.868 |
| Weibull | $\ln \left[-\ln \left(1 - \frac{Q_t}{Q_0} \right) \right]$ $= -\ln a + b \ln (t - t_0)$ $, a = (t_d)^b$ | R^2 | 0.994 | 0.991 |
| | | RMSE | 1.182 | 1.133 |
| | | b | 0.955 | 1.064 |
| | | a | 131.46 | 33.245 |
| | | t_d | 165.43 | 300.245 |

The FTIR analysis of curcumin reveals a distinct and pronounced peak within the 3400–3550 cm^{-1} range, indicating the presence of free –OH groups (Fig. 5). These groups serve as the primary sites for hydrogen bond formation which aligns with previous research (Xie et al. 2011). Upon the introduction of Tween 80, the sharp peak at 3508 cm^{-1} diminishes the intensity, supplanted by the emergence of a broader band spanning 3050–3555 cm^{-1} . This alteration is indicative of hydrogen bond formation (Sharma and Pathak 2016). Additionally, with the inclusion of Aerosil 200 in the optimized formulation, the sharp –OH stretching vibration vanishes entirely, replaced by a broadband that extends across the wider range of 3050–3780 cm^{-1} . This transformation signifies the substitution of weaker hydrogen bonds with stronger ones following the addition of Aerosil 200 (Kaushal et al. 2008). A similar observation was made by Planinšek et al. (Planinšek et al. 2011), who investigated the interaction between the drug and excipients. They reported that the formation of robust hydrogen bonds leads to the breakdown of weaker ones, playing a pivotal role in augmenting drug release from the system. In summary, it is evident that both Tween 80 and Aerosil 200 contribute positively to enhancing the dissolution of curcumin in the proposed liquisolid formulation.

In vitro dissolution studies

The dissolution profiles of curcumin liquisolid tablets (F1–F11) and the conventional tablet (F12) are depicted in Fig. 6. Comparatively, the curcumin liquisolid tablets, formulated with varying quantities of Tween 80 as the liquid vehicle and Aerosil 200 as the coating material, exhibited significantly higher drug dissolution rates ($P < 0.05$) in the 30 min compared to F12. Specifically, the average percentage of curcumin released from F1–F11 in

phosphate buffer within 30 min was 15.7%, whereas F12 showed a maximum drug release of 9.3% at the same time point. This observation can be attributed to the conversion of curcumin to a loss of crystallinity upon dispersion in the liquid vehicle, as indicated by the results of the DSC test. As reported by Badve et al., there's an electrostatic interaction between curcumin and Tween 80, which further elucidates the mechanism behind curcumin's enhanced solubility in the presence of Tween 80 (Badve and Pimpalkar 2023). Moreover, in liquisolid formulations, the drug particles are dispersed within a chosen hydrophilic liquid vehicle, enhancing the wetting properties of the drug particles. This greatly amplifies the available surface area for dissolution. Upon liquisolid tablet disintegration, the primary particles of the liquisolid remain suspended in the dissolution medium, housing drug particles in a state of molecular dispersion. Conversely, conventional tablets have limited surface exposure to dissolution due to the hydrophobic nature of the drug particles. The higher dissolution rates observed in liquisolid formulations are due to the significantly expanded surface area of the molecularly dispersed drug particles. Furthermore, in liquisolid formulations, the drug particles are molecularly dispersed, which could potentially elevate their saturation concentration. This increase in saturation concentration directly contributes to the enhanced drug release observed in these formulations, as demonstrated by the Noyes–Whitney equation (Kala et al. 2014; Souza Ferreira and Bruschi 2019; Vemula et al. 2010; Javadzadeh et al. 2007; Lu et al. 2017; Sirisolla 2015).

Although the CCD prediction suggested that F4 should be selected as the optimized formulation, Fig. 6 illustrates that F1 exhibited higher dissolution rates compared to F4. This can be attributed to their elevated concentration of Tween 80 (as indicated in Table 2). This observation is supported

by Eq. 9, demonstrating an increase in solubility with higher amounts of Tween 80. However, the selection of an optimized formulation encompasses a comprehensive evaluation of various critical tablet properties. For instance, the hardness of F1 was measured to be 36.27 N, significantly lower than the 52.93 N observed for F4. In addition, a similarity factor (f_2) test, as described in reference (Pawar et al. 2017), was conducted to compare the dissolution profiles of F12 and F4. The results indicated a significant difference, with the f_2 value being below 50. This confirms that the dissolution profile of F4 is significantly superior to that of F12.

According to CCD, the central point runs showed optimum results. So, the average drug release data from the three central runs were calculated, and mathematical models were investigated to find the best-fit model (a model with the highest R^2 and the lowest RMSE). According to Table 5, the release data followed the Weibull model.

The shape factor (b) was calculated to be 0.955 ($b < 1$), indicating that the release started with a steep initial slope. In the case of F12, the factor was 1.064 ($b > 1$) which means curcumin was released by super case-II transport. In this model, the release rate depends on the erosion of the matrix in which the drug is dispersed. In other words, tablet disintegration is a rate-limiting step in drug release for F12 formulation. The 3D surface graph (Fig. 3b) shows that the presence of Tween 80 in the formulation can improve disintegration time. This indicates that the liquid carrier can enhance the drug release rate in this way. The time-scale parameter (a) is an informative factor defined as t_d , $a = (t_d)^b$, where t_d is the time required for 63.2% of drug release (Farmoudeh et al. 2022). Based on the calculations, T_d was 165 min and 300 min for the optimized formulation (F4) and F12, respectively. Thus, a longer time was required for F12 to release 63.2% of the drug into the dissolution medium.

While other studies have explored various delivery systems such as liposomes (Xu et al. 2018), niosomes (Alemi et al. 2017) and polymeric nanoparticles (Orunoğlu et al. 2017) to address the limited solubility and poor bioavailability of curcumin (this restricts its clinical efficacy), our study introduces a simpler and cost-effective approach. The liquisolid technique demonstrated in this research not only offers an economical alternative, but also effectively enhances the dissolution rate of curcumin. This suggests that despite the sophistication of nano-based delivery systems, the liquisolid method remains a viable and potent solution for improving the solubility and potentially the therapeutic performance of curcumin. Furthermore, the implications of our findings are substantial for the development of various dosage forms for curcumin. In the case of curcumin tablets, if a high concentration of Tween 80 and a low concentration of Aerosil 200 are used, this

could potentially lead to more effective oral therapies by ensuring that the tablets can have adequate hardness, rapid dissolution and appropriate disintegration times, which are crucial for therapeutic efficacy of tablet formulation. In terms of powders, the liquisolid technique generally aims to convert hydrophobic solid drugs into dry, free-flowing powders. The flowability tests conducted in this study (Hausner's ratio, Carr's index, and angle of repose) show promising results, suggesting this technique could be extended to create powders that can be encapsulated or used in sachets. Manipulating the physical properties of the powders through the concentrations of Tween 80 and Aerosil 200 can tailor the release profiles and stability of the drug, resulting in powders that are easy to handle, store, and administer, making them a convenient dosage form for both patients and healthcare providers. For suspensions, the principles observed in this study can inform the development of liquid formulations where maintaining the drug in a molecularly dispersed state can significantly enhance absorption and bioavailability.

Conclusions

Curcumin, known for its poor water solubility and less than 1% oral bioavailability, poses a significant challenge for effective drug delivery. In this study when curcumin is dispersed in Tween 80 as the liquid vehicles, curcumin solid state was changed from a crystalline solid to a molecularly dispersed state which was confirmed by DSC results. This molecular dispersion enhances the solubility and dissolution rates of the drug in the dissolution medium. This underscores the potential of a liquisolid drug delivery system as a promising approach to address the poor dissolution rate of curcumin. For a better understanding of factors affecting the pharmaceutical properties of liquisolid formulations, CCD and RSM were employed. The study demonstrates a direct correlation between the concentrations of Tween 80 and Aerosil 200 with tablet hardness, dissolution at 30 min, and disintegration time. Specifically, Tween 80 significantly enhances solubility and dissolution, while Aerosil 200's increase correlates with decreased tablet hardness and slower dissolution rates. Furthermore, the in vitro dissolution profiles clearly indicate superior dissolution rates for all liquisolid formulations compared to the conventional formulation (F12). Significantly, formulation F4, positioned as a central point in the CCD design and comprising 30 mg of Tween 80 along with 75 mg of Aerosil 200, emerged as the optimized choice. This determination was grounded in CCD predictions and validated through experimental evaluations, considering critical parameters such as tablet hardness, dissolution at 30 min, and disintegration time across the 12 formulations studied. Moreover, upon comparing various

mathematical models, the release data followed the Weibull model.

While alternative nano-based delivery systems such as liposomes and nanoparticles have been explored to address curcumin's solubility and bioavailability issues, our study introduces the liquisolid technique as a simpler and cost-effective solution to improve the dissolution rate of curcumin. This method not only enhances the dissolution rate of curcumin, but also shows significant promise in developing various dosage forms, including tablets with improved hardness and rapid dissolution, and free-flowing powders suitable for encapsulation. These findings underscore the potential of the liquisolid system to improve drug delivery for curcumin. However, for a comprehensive understanding of the potential of liquisolid for curcumin, further studies encompassing animal and human pharmacokinetics and pharmacodynamics are imperative. These endeavors will provide critical insights into the translational potential of this formulation approach.

Author contribution Sareh Aghajanzpour involved in methodology, software, validation, formal analysis, investigation, and writing—original draft; Shabnam Yousefi Jordehi involved in methodology, investigation, and formal analysis; Ali Farmoudeh involved in methodology, investigation, and formal analysis; Reza Negarandeh involved in methodology, investigation, and writing—original draft; Matthew Lam involved in formal analysis and writing—review and editing; Pedram Ebrahimnejad involved in conceptualization, resources, writing—original draft, writing—review and editing, supervision, and project administration; Ali Nokhodchi involved in formal analysis and writing—review and editing.

Declarations

Conflict of interest The authors declare no conflict of interest.

Open Access This article is licensed under a Creative Commons Attribution 4.0 International License, which permits use, sharing, adaptation, distribution and reproduction in any medium or format, as long as you give appropriate credit to the original author(s) and the source, provide a link to the Creative Commons licence, and indicate if changes were made. The images or other third party material in this article are included in the article's Creative Commons licence, unless indicated otherwise in a credit line to the material. If material is not included in the article's Creative Commons licence and your intended use is not permitted by statutory regulation or exceeds the permitted use, you will need to obtain permission directly from the copyright holder. To view a copy of this licence, visit <http://creativecommons.org/licenses/by/4.0/>.

References

- Abo-Zaid MA, Shaheen ES, Ismail AH (2020) Immunomodulatory effect of curcumin on hepatic cirrhosis in experimental rats. *J Food Biochem* 44(6):e13219
- Ahmadi F, Akbari J, Saeedi M, Seyedabadi M, Ebrahimnejad P, Ghasemi S, Nokhodchi A (2023) Efficient synergistic combination effect of curcumin with piperine by polymeric magnetic nanoparticles for breast cancer treatment. *J Drug Delivery Sci Technol* 8:104624
- Ainurofiq A, Choiri S, Azhari MA, Siagian CR, Suryadi BB, Priharsara F, Rohmani S (2016) Improvement of meloxicam solubility using a β -cyclodextrin complex prepared via the kneading method and incorporated into an orally disintegrating tablet. *Adv Pharm Bull* 6(3):399
- Alemi A, Farrokhifar M, Karamallah MH, Farrokhifar M, Nasab ZE, Farrokhifar A (2017) Evaluation of the efficacy of niosomal curcumin nanoformulation in cancer therapy. *Cancer Press* 3(3):77–85
- Anand P, Kunnumakkara AB, Newman RA, Aggarwal BB (2007) Bioavailability of curcumin: problems and promises. *Mol Pharm* 4(6):807–818
- Badve M, Pimpalkar M (2023) Efficacy of curcumin-surfactant complex towards stabilisation of emulsions. *Trans Indian Natl Acad Eng* 8(1):127–137
- Basnet P, Skalko-Basnet N (2011) Curcumin: an anti-inflammatory molecule from a curry spice on the path to cancer treatment. *Molecules* 16(6):4567–4598
- Beg S, Katare OP, Singh B (2017) Formulation by design approach for development of ultrafine self-nanoemulsifying systems of rosuvastatin calcium containing long-chain lipophiles for hyperlipidemia management. *Colloids Surf B* 1(159):869–879
- Biswas A, Das P, Mandal NK (2017) Factorial designs robust against the presence of an aberration. *Statist Probab Lett* 1(129):326–334
- Choiri S, Ainurofiq A, Ratri R, Zulmi MU (2018) Analytical method development of nifedipine and its degradants binary mixture using high performance liquid chromatography through a quality by design approach. *InIOP Conference Series: Materials Science and Engineering* 2018 Mar 1 (Vol. 333, No. 1, p. 012064). IOP Publishing.
- Cui Z, Yao L, Ye J, Wang Z, Hu Y (2021) Solubility measurement and thermodynamic modelling of curcumin in twelve pure solvents and three binary solvents at different temperature ($T = 278.15$ – 323.15 K). *J Mol Liquids* 15(338):116795
- de Souza Ferreira SB, Bruschi ML (2019) Improving the bioavailability of curcumin: is micro/nanoencapsulation the key? *Ther Deliv* 10(2):83–86
- Den Hartogh DJ, Gabriel A, Tsiani E (2020) Antidiabetic properties of curcumin I: evidence from in vitro studies. *Nutrients* 12(1):118
- Esezobo S (1985) The effect of some excipients on the physical properties of a paracetamol tablet formulation. *J Pharm Pharmacol* 37(3):193–195
- Farmoudeh A, Saeedi M, Talavaki F, Ghasemi M, Akbari J, Nokhodchi A (2022) Methylene blue loaded solid lipid nanoparticles: Preparation, optimization, and in-vivo burn healing assessment. *J Drug Delivery Sci Technol* 1(70):103209
- Ghadi ZS, Dinarvand R, Asemi N, Amiri FT, Ebrahimnejad P (2019) Preparation, characterization and in vivo evaluation of novel hyaluronan containing niosomes tailored by Box-Behnken design to co-encapsulate curcumin and quercetin. *Eur J Pharm Sci* 15(130):234–246
- Ghadi ZS, Ebrahimnejad P (2017) Niosome, a novel drug delivery system, for improving therapeutic efficacy of curcumin. *20th Iranian Pharmacy Students Seminar (IPSS) 2017*. 6:1436. <https://doi.org/10.7490/f1000research.1114690.1>
- Giordano A, Tommonaro G (2019) Curcumin and cancer. *Nutrients* 11(10):2376
- Górnicka J, Mika M, Wróblewska O, Siudem P, Paradowska K (2023) Methods to improve the solubility of curcumin from turmeric. *Life* 13(1):207
- Hamaguchi T, Ono K, Yamada M (2010) Curcumin and Alzheimer's disease. *CNS Neurosci Ther* 16(5):285–297

- Heng PW, Wan LS, Ang TS (1990) Role of surfactant on drug release from tablets. *Drug Dev Ind Pharm* 16(6):951–962
- Hewlings SJ, Kalman DS (2017) Curcumin: a review of its effects on human health. *Foods* 6(10):92
- Hezarjaribi HZ, Mollarostami F, Ebrahimnejad P, Esboei BR, Fakhar M, Sadeghi-Ghadi Z (2022) Promising potent in vitro activity of curcumin and quercetin nano-niosomes against *Trichomonas vaginalis*. *Annal Parasitol* 68(2):263–273
- Hu RW, Carey EJ, Lindor KD, Tabibian JH (2018) Curcumin in hepatobiliary disease: pharmacotherapeutic properties and emerging potential clinical applications. *Ann Hepatol* 16(6):835–841
- Javadzadeh Y, Jafari-Navimipour B, Nokhodchi A (2007) Lquisolid technique for dissolution rate enhancement of a high dose water-insoluble drug (carbamazepine). *Int J Pharm* 341(1–2):26–34
- Juppo A, Yliruusi J, Kervinen L (1991) The effect of compression pressure and compression speed on disintegration time and tensile strength of lactose, glucose and mannitol tablets. In *Proceedings of 10th Pharmaceutical Technology Conference: Vol 1 1991* (pp. 558–567).
- Kala NP, Shaikh MT, Shastri DH, Shelat PK (2014) A Review on liquisolid systems. *J Drug Delivery Ther* 4(3):25–31
- Kaushal AM, Chakraborti AK, Bansal AK (2008) FTIR studies on differential intermolecular association in crystalline and amorphous states of structurally related non-steroidal anti-inflammatory drugs. *Mol Pharm* 5(6):937–945
- Kumar A, Singh M, Singh PP, Singh SK, Raj P, Pandey KD (2016) Antioxidant efficacy and curcumin content of turmeric (*Curcuma longa* L.) flower. *Int J Current Pharm Res* 1:112–4
- Kumar PR, Chaitanya P, Kalyani R, Poojitha RM, Bhavani U, Rao ST (2019) Formulation and evaluation of curcumin liquisolid tablets. *JPI* 8:368–374
- Li H, Jiang Y, Yang J, Pang R, Chen Y, Mo L, Jiang Q, Qin Z (2023) Preparation of curcumin-chitosan composite film with high antioxidant and antibacterial capacity: Improving the solubility of curcumin by encapsulation of biopolymers. *Food Hydrocolloids* 1(145):109150
- Lu M, Xing H, Jiang J, Chen X, Yang T, Wang D, Ding P (2017) Liquisolid technique and its applications in pharmaceuticals. *Asian J Pharm Sci*. 12(2):115–23
- Nabavi SF, Daglia M, Moghaddam AH, Habtemariam S, Nabavi SM (2014) Curcumin and liver disease: from chemistry to medicine. *Compr Rev Food Sci Food Safety* 13(1):62–77
- Negi PS, Jayaprakasha GK, Jagan Mohan Rao L, Sakariah KK (1999) Antibacterial activity of turmeric oil: a byproduct from curcumin manufacture. *J Agric Food Chem* 47(10):4297–300
- Obeid MA, Alsaadi M, Aljabali AA (2023) Recent updates in curcumin delivery. *J Liposome Res* 33(1):53–64
- Ohta KM, Fuji M, Takei T, Chikazawa M (2003) Effect of geometric structure and surface wettability of glidant on tablet hardness. *Int J Pharm* 262(1–2):75–82
- Orunoğlu M, Kaffashi A, Pehlivan SB, Şahin S, Söylemezoğlu F, Oğuz KK, Mut M (2017) Effects of curcumin-loaded PLGA nanoparticles on the RG2 rat glioma model. *Mater Sci Eng C* 1(78):32–38
- Parrott EL (1981) Compression. In: Lieberman HA, Lachman L (eds) *Pharmaceutical dosage forms: tablets*, vol 2. Marcel Dekker, New York, pp 153–184
- Pawar JD, Jagtap RS, Doijad RC, Pol SV, Desai JR, Jadhav VV, Jagtap SR (2017) Liquisolid compacts: a promising approach for solubility enhancement. *J Drug Delivery Ther* 7(4):6–11
- Planinšek O, Kovačič B, Vrečer F (2011) Carvedilol dissolution improvement by preparation of solid dispersions with porous silica. *Int J Pharm* 406(1–2):41–48
- Rathore S, Mukim M, Sharma P, Devi S, Nagar JC, Khalid M (2020) Curcumin: a review for health benefits. *Int J Res Rev* 7(1):273–290
- Ravichandran R (2013) Studies on dissolution behaviour of nanoparticulate curcumin formulation. *Adv Nanoparticles* 2(01):51–59
- Sadeghi Ghadi Z, Ebrahimnejad P (2019) Curcumin entrapped hyaluronan containing niosomes: preparation, characterisation and in vitro/in vivo evaluation. *J Microencapsul* 36(2):169–179
- Sadeghi-Ghadi Z, Vaezi A, Ahangarkani F, Ilkit ME, Ebrahimnejad P, Badali H (2020) Potent in vitro activity of curcumin and quercetin co-encapsulated in nanovesicles without hyaluronan against *Aspergillus* and *Candida* isolates. *J De Mycol Med* 30(4):101014
- Sadeghi-Ghadi Z, Behjou N, Ebrahimnejad P, Mahkam M, Goli HR, Lam M, Nokhodchi A (2023) Improving antibacterial efficiency of curcumin in magnetic polymeric nanocomposites. *J Pharm Innov* 18(1):13–28
- Saeedi M, Akbari J, Semnani K, Hashemi SM, Ghasemi S, Tahmasbi N, Azizpoor E, Faghani N, Rostamkalaei SS, Nokhodchi A (2022) Controlling atorvastatin release from liquisolid systems. *J Dispersion Sci Technol* 43(3):375–384
- Sander C, Holm P (2009) Porous magnesium aluminometasilicate tablets as carrier of a cyclosporine self-emulsifying formulation. *AAPS PharmSciTech* 10(4):1388–1395
- Sanka K, Poienti S, Mohd AB, Diwan PV (2014) Improved oral delivery of clonazepam through liquisolid powder compact formulations: in-vitro and ex-vivo characterization. *Powder Technol* 1(256):336–344
- Sharma V, Pathak K (2016) Effect of hydrogen bond formation/replacement on solubility characteristics, gastric permeation and pharmacokinetics of curcumin by application of powder solution technology. *Acta Pharm Sinica b* 6(6):600–613
- Sirisolla J (2015) Solubility enhancement of meloxicam by liquisolid technique and its characterization. *Int J Pharm Sci Res* 6(2):835
- Solanki SS, Paliwal P, Jain S, Sharma P, Sarkar B (2012) Formulation and evaluation of curcuminliquisolid tablets. *Current Res Pharm Sci* 31:210–214
- Spireas S, Sadu S (1998) Enhancement of prednisolone dissolution properties using liquisolid compacts. *Int J Pharm* 166(2):177–188
- Tiong N, Elkordy AA (2009) Effects of liquisolid formulations on dissolution of naproxen. *Eur J Pharm Biopharm* 73(3):373–384
- United States Pharmacopeia (2022) *United States Pharmacopeia and National Formulary (USP-NF)*, Rockville, MD, USA: 2022. General Chapter, {1217} Tablet Breaking Force
- United States Pharmacopeial Convention (2019) *United States Pharmacopeia and National Formulary (USP 43-NF 38)*, <701> Disintegration. Rockville, MD: United States Pharmacopeia
- United States Pharmacopeial Convention (2020) *United States Pharmacopeia and National Formulary (USP/NF, 2020e)*, General chapters: {1216} Tablet Friability. 43rd ed. Vol. 31(6). Rockville, MD: United States Pharmacopeia; p. 8137
- Vemula VR, Lagishetty V, Lingala S (2010) Solubility enhancement techniques. *Int J Pharm Sci Rev Res* 5(1):41–51
- Wei TK, Manickam S (2012) Response Surface Methodology, an effective strategy in the optimization of the generation of curcumin-loaded micelles. *Asia-Pac J Chem Eng* 7:S125–S133
- Xie X, Tao Q, Zou Y, Zhang F, Guo M, Wang Y, Wang H, Zhou Q, Yu S (2011) PLGA nanoparticles improve the oral bioavailability of curcumin in rats: characterizations and mechanisms. *J Agric Food Chem* 59(17):9280–9289
- Xu H, Gong Z, Zhou S, Yang S, Wang D, Chen X, Wu J, Liu L, Zhong S, Zhao J, Tang J (2018) Liposomal curcumin targeting endometrial cancer through the NF-κB pathway. *Cell Physiol Biochem* 48(2):569–582
- Yan FS, Sun JL, Xie WH, Shen L, Ji HF (2017) Neuroprotective effects and mechanisms of curcumin–Cu (II) and–Zn (II) complexes systems and their pharmacological implications. *Nutrients* 10(1):28
- Yang C, Zhu K, Yuan X, Zhang X, Qian Y, Cheng T (2020) Curcumin has immunomodulatory effects on RANKL-stimulated osteoclastogenesis in vitro and titanium nanoparticle-induced bone loss in vivo. *J Cell Mol Med* 24(2):1553–1567

Publisher's Note Springer Nature remains neutral with regard to jurisdictional claims in published maps and institutional affiliations.